



Evaluation of comfort zone boundary based automated emergencybraking algorithms for car-to-powered-two-wheeler crashes inChina


Downloaded from: <https://research.chalmers.se>, 2024-08-16 10:36 UTC

Citation for the original published paper (version of record):

Yang, X., Lübbe, N., Bärgerman, J. (2024). Evaluation of comfort zone boundary based automated emergencybraking algorithms for car-to-powered-two-wheeler crashes inChina. IET Intelligent Transport Systems, In press. <http://dx.doi.org/10.1049/itr2.12532>

N.B. When citing this work, cite the original published paper.

Evaluation of comfort zone boundary based automated emergency braking algorithms for car-to-powered-two-wheeler crashes in China

Xiaomi Yang¹  | Nils Lubbe^{1,2} | Jonas Bårgman¹

¹Division of Vehicle Safety at the Department of Mechanics and Maritime Sciences, Chalmers University of Technology, Gothenburg, Sweden

²Autoliv Research, Vårgårda, Sweden

Correspondence

Xiaomi Yang, Division of Vehicle Safety at the Department of Mechanics and Maritime Sciences, Chalmers University of Technology, Hörselgängen 4, Gothenburg 417 56, Sweden.
Email: xiaomi.yang@chalmers.se

Funding information

European Commission under Marie Skłodowska-Curie grant agreement, Grant/Award Number: 860410; Autoliv Development AB

Abstract

Crashes between cars and powered two-wheelers (PTWs: motorcycles, scooters, and e-bikes) are a safety concern; as a result, developing car safety systems that protect PTW riders is essential. While the pre-crash protection system automated emergency braking (AEB) has been shown to avoid and mitigate injuries for car-to-car, car-to-cyclist, and car-to-pedestrian crashes, much is still unknown about its effectiveness in car-to-PTW crashes. Further, the characteristics of the crashes that remain after the introduction of such systems in traffic are also largely unknown. This study estimates the crash avoidance and injury risk reduction performance of six different PTW-AEB algorithms that were virtually applied to reconstructed car-to-PTW pre-crash kinematics extracted from a Chinese in-depth crash database. Five of the algorithms include combinations of drivers' and PTW riders' comfort zone boundaries for braking and steering, while the sixth is a traditional AEB. Results show that the average safety performance of the algorithms using only the driver's comfort zone boundaries is higher than that of the traditional AEB algorithm. All algorithms resulted in similar distributions of impact speed and impact locations, which means that in-crash protection systems likely can be made less complex, not having to consider differences in AEB algorithm design among car manufacturers.

1 | INTRODUCTION

In Southeast Asia, powered two- and three-wheelers are a critical safety concern: their riders account for 43% of all traffic deaths there [1]. The majority of these vehicles are powered two-wheelers (PTWs): motorcycles, scooters, and e-bikes [2], powered either by an electric engine (using rechargeable batteries) or a combustion engine. Statistics from 2022 indicate that there were 9,923 fatalities and 48,518 traffic injuries involving motorcycles alone reported in China, often in collisions with cars [3].

Systems addressing car-to-PTW safety can be classified into in-crash and pre-crash systems. The former seek to prevent or mitigate injuries when crashes occur [4, 5], while the latter seek to avoid the crash altogether or mitigate its consequences—by reducing the impact speed before the crash [6], for example, automated emergency braking (AEB) [7–9], an intelligent

transport system currently available in production vehicles, is a pre-crash protection system; it triggers vehicle braking automatically in critical situations.

Several studies have shown that AEB systems substantially prevent or mitigate injuries in car-to-car crashes [10, 11], car-to-pedestrian crashes [12, 13], and car-to-cyclist crashes [14–16]. Although some information about car-to-car rear-end and intersection AEBs can be inferred from the literature [10, 11, 17], very little is known about AEB systems specifically targeting car-to-PTW crashes (hereafter called PTW-AEB systems); only a few studies have investigated their potential benefits. In one study, Dean et al. [18] investigated the potential benefits of a motorcycle-detecting AEB system; in another, based on French crash data, Saadé et al. [19] estimated the effectiveness of a PTW-AEB algorithm that triggered the AEB's activation at a fixed time to collision (TTC) of 1 s. Sui et al. [20] estimated a safety benefit of approximately 46% crash avoidance in China

This is an open access article under the terms of the [Creative Commons Attribution -NoDerivs License](https://creativecommons.org/licenses/by/4.0/), which permits use and distribution in any medium, provided the original work is properly cited and no modifications or adaptations are made.

© 2024 The Author(s). *IET Intelligent Transport Systems* published by John Wiley & Sons Ltd on behalf of The Institution of Engineering and Technology.

for a TW-AEB that activates braking at a fixed TTC of 1.1 s. Lastly, Zhao et al. [21] reported that the effectiveness of a Honda in-production AEB for two Chinese car-to-TW crash scenarios ranges from 41% to 75%, depending on radar detection range and scenario type. Although these studies provide some insights, there is a need for more quantitative comparisons of the influence of different AEB algorithm designs on car-to-TW crashes—not only to determine what types and how many of crashes are likely to be successfully prevented, but also to study the characteristics of the crashes that are likely to remain.

Information about these ‘residual’ or ‘remaining’ crashes [22–24] can help the automotive industry, policy makers, consumer rating programs [25], and researchers target the development and assessment of the next generation of safety systems: in-crash protection systems will have to prevent these crashes after the ubiquity of PTW-AEBs has made other types of crashes much less common. However, the characteristics of these remaining crashes have not yet been reported in the literature (for China or elsewhere) [26].

The timing of the activation of the pre-crash safety system (here PTW-AEB) clearly plays a large role in which crashes remain, as well as in the system’s overall effectiveness. Importantly, the algorithm logic differs substantially between systems—car manufacturers have proprietary AEB algorithms. Early versions of car-to-car AEB considered only some threshold for the time to collision (TTC), while more current AEB systems have much more elaborate algorithm designs: instead of TTC they might calculate the level of braking (deceleration, the negative acceleration when a car brakes) required to avoid a crash [27], or they might include assumptions about what the driver can comfortably do to avoid a crash [28]. Thus, it is important to thoroughly assess each specific system when performing a quantitative safety benefit assessment. If the specific algorithm’s logic results in remaining crashes with different characteristics than those of other systems, then the design of in-crash protection systems may become more complex and expensive (since they may have to be tuned to address the remaining crashes of the specific pre-crash system).

The required-deceleration AEB algorithm [27] is a common approach which uses the concept of a ‘point of no return’ beyond which it would be physically impossible to brake hard enough to avoid a crash. If the system brakes before that point, the driver may still be able to avoid the crash by braking or steering; in fact, even after this point the driver may still be able to steer away comfortably (in an overtaking manoeuvre, for example). As a result, the required-deceleration algorithm might activate too early, resulting in nuisance (false positive) interventions, which may impact driver acceptance of the system [26, 29, 30].

This issue can be resolved if the algorithm assesses whether the driver can avoid a collision through comfortable braking or steering, not just by maximum braking by the AEB [28]. That is, instead of simply considering the point of no return, the AEB algorithm can be designed to consider the driver’s comfort zone (CZ) and its boundaries (CZB; Summala [31]). When drivers

are in their CZ, they feel comfortable, and safety system interventions are typically not appreciated; on the other hand, when they exceed the CZB, they no longer feel at ease and would likely accept safety system interventions in order to return to their CZ. Incorporating CZBs into AEB algorithms can enable brake activation earlier than the point of no return, resulting in reduced crash and injury risks, while avoiding brake activation if the driver (or the other road user) could still avoid a potential crash in a comfortable way, even after the point of no return for braking. If the intervention is triggered after the driver’s CZB has been crossed (i.e. where the driver would feel discomfort), then the driver is likely to consider the system activation helpful rather than a nuisance [32]. However, when the driver’s CZB is beyond the point of no return for braking, an intervention at the point of no return for braking may be perceived as a nuisance, possibly warranting a delay in the intervention until the CZB is reached. Clearly, AEBs need to have values for comfortable levels of longitudinal (braking) acceleration and lateral (steering) acceleration in order to make use of CZBs. Fortunately, such values have been established for drivers [33, 34]. The use of CZBs in safety system algorithms has been championed by, for example, Sander [35], Bärgrman [33], and Brännström et al. [36]. Their research, in turn, was based on work by Gibson and Crooks [37] and Summala [30].

Currently, however, it is unknown how different combinations of CZBs affect the crash avoidance performance of PTW-AEB algorithms—or the characteristics of the remaining crashes in car-to-PTW conflicts. This study intends to address these two research gaps.

One common way to assess the benefit of a system such as AEB is to use virtual counterfactual simulations [28, 38–40], which apply the safety system under study to virtual representations of actual crashes (which originally involved cars without the safety system). Comparing the actual and simulated outcomes provides an estimate of the system’s effectiveness. Typically, the results include the proportion of avoided crashes and the impact speeds—and sometimes, injury reduction estimates [20]. A main source of data for virtual simulations are reconstructions of the pre-crash kinematics of actual crashes in in-depth crash databases [28, 35, 40, 41]. One in-depth database that contains car-to-PTW crashes in China is the Shanghai United Road Traffic Safety Scientific Research Center (SHUFO) database. SHUFO records crashes involving passenger cars in Shanghai, China. The SHUFO selection criteria require that the crash result in injuries or high economic loss [42]. More details on SHUFO, including an assessment of its representativity, can be found in the work by Zhao et al. [17].

There are two aims of this study. The first is to compare the performance of five different PTW-AEB algorithms which have different combinations of comfortable crash avoidance manoeuvres against each other as well as against a more traditional PTW-AEB algorithm. These comparisons may help improve future PTW-AEB designs, because AEBs with CZB-based algorithms may trigger earlier than more basic, traditional algorithms which rely on maximum deceleration. Critically, the CZB-based algorithms’ interventions would not be perceived as

a nuisance. On the other hand, these algorithms in some cases would enable triggering later than the traditional AEB when comfortable steering is still a way to avoid the crash—even when maximum braking is not.

The second aim is to characterize the remaining crashes that are likely to remain after PTW-AEB is commonly available in cars in China. Their characteristics can be used by the automotive industry and C-NCAP to further refine PTW-AEBs—but even more importantly, to define future in-crash protection needs. Differences (or similarities) in crash characteristics across the algorithms can provide insights into the need for tuning in-crash protection systems. Further, automated driving systems may also use CZB-based algorithm designs to improve crash avoidance and injury risk reduction performance and reduce nuisance interventions. These aims were accomplished by applying virtual representations of the six AEB systems to the pre-crash kinematics from reconstructed SHUFO crashes. The algorithms were compared in terms of the trigger timing, proportion of avoided crashes, injury risk reduction, and impact speed reduction.

2 | METHODS

2.1 | Data

We first selected the 263 crashes with only one car and one PTW from the total of 930 SHUFO crashes collected between 2011 and 2018. Of the original 263, 157 lacked the necessary data (e.g. no dynamics data available, corrupt data), so 106 were reconstructed in the PCTSD (pre-crash time-series data) format by Autoliv researchers, who used reconstruction software to calculate additional relevant metrics from the available data (see Sui et al. [20] for more details). A further 13 crashes were eliminated because the duration of the reconstructed crash was too short. Thus the data from 93 crashes were finally used. The data follow the content and structure of GIDAS PCM data [43]. In addition to the participant data metrics (weight, length, width, and wheelbase of passenger cars and PTWs) from the original SHUFO crashes, the following metrics from the reconstructed PCTSD data were used: velocity, acceleration, position, heading angle, and yaw angle—as well as the road friction coefficient, used for calculating the car's maximum braking capacity. (Descriptions of the metrics can be found in Appendix C.) In the preparatory stages of the study, we divided the cases into nine different scenarios, but due to the low number of crashes in several scenarios we present the 93 crashes as a single dataset in this paper. However, the distribution across the scenarios, the description of the scenario classifications, and the estimated AEB performance of each scenario can be found in Appendix A.

Of the 93 SHUFO crashes used in this paper, 12.6% of the PTWs are scooters and 4.9% are heavy motorcycles, with median estimated driving speeds of 30.0 km/h (mean: 29.9 km/h) and 30.0 km/h (mean: 32.8 km/h), respectively. The remaining 82.5% of the PTWs are e-bikes, with a median speed of 20.0 km/h (mean: 18.1 km/h). The data frequency is 100 Hz (0.01 s simulation time step).

2.2 | Simulation framework

In the simulation framework (based on Rosén [15] and Yang [44]), the car and PTW are modelled as 2D shapes which follow the original trajectories (the shape parameters can be found in Appendix C). For the sake of simplicity, lateral and vertical dynamics are not modelled, and it is assumed that the sensors made perfect recognition and position estimates. That is, the sensors are considered ideal, as is often the case in virtual simulations [45] but not in the real world [46]. Finally, the braking trigger time (the time from the start of the simulation until the AEB is triggered) for each reconstructed crash was simulated according to the AEB algorithm applied.

2.3 | AEB algorithms

2.3.1 | AEB algorithm variations

We implemented and compared two AEB algorithm concepts: TAEB (Traditional AEB) and CAEB (CZB-based AEB). The TAEB uses the required-deceleration algorithm based on the point of no return, by braking with the car's maximum braking ability at the last possible moment to avoid a crash. The five CAEB algorithms, on the other hand, all include some combination of comfortable braking and/or steering manoeuvres of the driver and rider. Consider, for example, an algorithm (CZ: 'Driver brake') that incorporates the driver's comfortable braking: at each time step (of 0.01s) in the simulation, the algorithm predicts whether the involved road users would crash if the driver brakes at the longitudinal CZB. (In physical terms, the CZB lies at the level of longitudinal deceleration beyond which the driver feels uncomfortable.) Note that this CAEB triggers earlier than the TAEB, because comfortable deceleration requires more distance (and time) to avoid the crash than the maximum deceleration assumed by the TAEB.

Now consider an algorithm that also incorporates the driver's comfortable steering: at each time step, the algorithm predicts whether the involved road users will crash if the driver steers away in a comfortable manner (within his or her CZ in terms of lateral acceleration). The AEB would be triggered if the algorithm predicts that neither a comfortable braking manoeuvre nor a comfortable steering manoeuvre can avoid a crash. In the case of steering, the CZB is the absolute value of the lateral (centripetal) acceleration (induced by the speed and yaw rate of the vehicle) above which the driver feels uncomfortable. This algorithm (considering both comfortable steering and comfortable braking) triggers the AEB later than an algorithm considering braking comfort alone (Figure 1, top two algorithms).

The CZs (and corresponding CZBs) for the five CAEB algorithms are conceptually illustrated in Figure 1. It should be kept in mind that, when the AEB considers the rider's CZB it is actually applying the driver's 'idea' of the rider's CZB, as it is the nuisance of the driver that is to be considered. The same logic described above is used: the AEB does not brake if the driver (according to the CAEB's driver model) believes that the rider would be able to brake or steer comfortably. The AEB does not

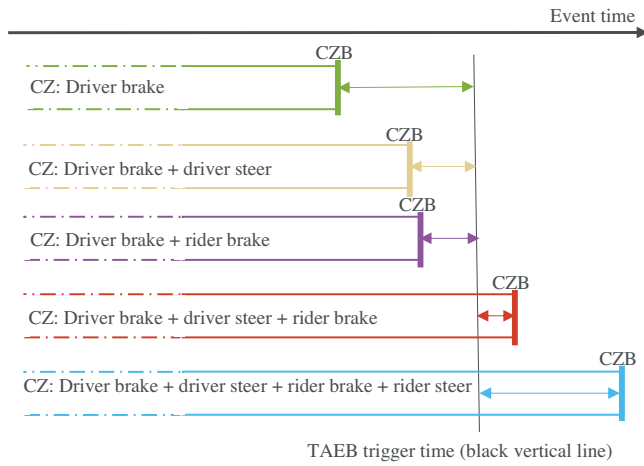


FIGURE 1 Illustration of CZBs. This figure shows the relative trigger timing of the six algorithms (conceptually). The combinations after CAEB describe the CZB AEB comfortable avoidance manoeuvres included in the algorithm. The CZs, the CZBs, and the TAEB and CAEB trigger times all differ across their application to the reconstructed crashes; see Appendix D for details.

TABLE 1 AEB algorithm variations.

CZB-based AEB algorithms	CAEB: Driver brake
	CAEB: Driver brake + driver steer
	CAEB: Driver brake + rider brake
	CAEB: Driver brake + driver steer + rider brake
Traditional AEB algorithm	CAEB: Driver brake + driver steer + rider brake + rider steer
	TAEB (required-deceleration-based)

trigger until the involved road users cannot avoid the crashes with any of the included comfortable avoidance options.

Note that Figure 1 is conceptual: until the simulations are performed and analysed, the exact timing is not known. However, given the way the CAEB algorithm logic works, it is possible to know the order of the CAEB algorithm trigger timings to some extent: the more options of comfortable avoidance included, the later the trigger. That is, starting with a single option (see CZ: ‘Driver brake’ at the top of Figure 1), the trigger times increase as the number of road users’ comfortable avoidance manoeuvre options increases. Note that ‘Driver brake + driver steer’ is illustrated as triggering slightly earlier than the ‘Driver brake + rider brake’, but that is just a conceptual illustration; they both use two avoidance manoeuvres, so it cannot be known before simulating which algorithm will actually trigger earlier.

Each of the six AEB algorithms (detailed in Table 1) was applied to each of the 93 original SHUFO crashes. In total, 558 individual simulations were thus performed. Results are collated per AEB algorithm.

The six algorithms all share the same path prediction logic, which requires the PTW to be within the car sensor’s field of view (FoV) and range. In this study, the FoV was 180° and

the range limit was 60 m, as used by Jeppsson et al. [12]. For more details on the rationale of sensor parameter selection, see Appendix B.

The logic for both the TAEB and CAEB algorithms is as follows: When the PTW is detected by the car’s sensors, the algorithm starts estimating the future paths of both the car and the PTW. At each time step, the algorithm checks for a potential collision (path intersection). The paths are calculated by extrapolating the dynamics (position, velocity, acceleration heading angle, and yaw angle; described in more detail in Appendix C) of the car and PTW. Using a simple vehicle dynamics model (the bicycle model [47]), the algorithm assumes that the car and PTW will continue driving with the current acceleration and curvature. If the predicted paths at one time step do not produce a crash, the simulation moves to the next time step, until the end of the data. Only when the predicted future paths result in a collision does the AEB algorithm determine if it should initiate braking according to its logic. The shapes of the car and the PTW used in the predictions and AEB algorithm designs are 1.5 times larger than the original shapes (see Appendix C), to allow for prediction errors and include driver safety margins. If and only if all of the conditions for that AEB are fulfilled are the vehicle brakes applied. For example, in CAEB: ‘Driver brake + rider brake’, if the driver or rider can brake comfortably and still avoid a crash, the AEB does not initiate the braking avoidance manoeuvre, even if the deceleration-only TAEB algorithm would initiate braking.

For each of the five CAEB algorithms, we also assessed a technically trivial variant which may trigger earlier than the TAEB (which triggers at the vehicle’s point of no return for braking), but never later. These variants are not intended to address nuisance warnings of TAEB. Rather, they focus on the safety benefit of algorithms that take CZBs into account: these algorithms never trigger later than the point of no return—while minimizing nuisance interventions.

2.3.2 | Braking and steering mechanism

The characteristics of the braking and steering profiles are the same for the five CAEB algorithms. For the braking profile, shown on the left in Figure 2, a constant jerk j_{\min} is applied. When that jerk produces braking equal to the minimum braking a_{\min} , that minimum value is maintained until the car or PTW stops (parameter settings can be found in Table 2). The braking vehicle (car or PTW) is assumed to travel in a straight line. Table 2 lists the comfortable braking parameter settings for the profiles used in this study (based on works by Brännström et al. [48], Kiefer et al [33], Bärnman et al. [34], and C-NCAP [49]). For the steering profile, the steering wheel angle is linearly increased (left or right) at a constant steering wheel angle rate $\dot{\theta}_c$ until it reaches the maximum steering wheel angle θ_c (see right panel in Figure 2). The angle θ_c is the angle at which the vehicle’s absolute lateral acceleration reaches the maximum absolute comfortable lateral acceleration a_{\max}^{lat} or the vehicle’s absolute lateral jerk reaches the maximum absolute comfortable jerk j_{\max}^{lat} , whichever occurs earlier. Table 3 lists the steering

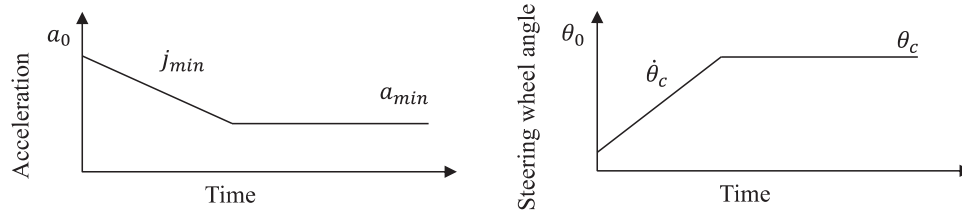


FIGURE 2 Parameterization of the braking (left) and steering (right) manoeuvres.

TABLE 2 Comfortable braking limits of car drivers and PTW riders and maximum braking limits of the car.

Parameters	Description	Car driver [33, 34, 48]	PTW [33, 34, 48]	Car
a_{min} (m/s ²)	Minimum comfortable brake acceleration*	-5	-5	-8.83 [49]
j_{min} (m/s ³)	Minimum comfortable brake jerk	-10	-10	-20 [48]

* Note that deceleration is the negative acceleration.

TABLE 3 Comfortable steering limits of drivers and PTW riders.

Parameters	Description	Car driver	PTW
a_{max}^{lat} (m/s ²)	Maximum absolute comfortable lateral acceleration due to steering	5 [33, 34, 48]	5 [33, 34, 48]
j_{max}^{lat} (m/s ³)	Maximum absolute comfortable lateral jerk due to steering	5 [48]	5 [33, 34, 48]
θ_c (°)	Maximum steering wheel angle	720 [48]	3 [50]
$\dot{\theta}_c$ (°/s)	Maximum comfortable steering wheel angle rate	400 [48]	3 [50]
Steering ratio	Steering ratio of the vehicle	15	1

parameter settings (based on works by Brännström et al. [48], Kiefer et al [33], Bårgman et al. [34], and Costa et al. [50]).

Because data about the driver’s ‘idea’ of PTW CZBs were not available for this study, the comfortable braking and steering levels for PTW riders are set to those of car drivers. To calculate the braking level of the vehicle in TAEB, a friction coefficient of 0.9 is assumed, based on the testing protocol of PTW-AEB assessment in C-NCAP [51].

2.4 | Analysis

The algorithms’ performances were compared using the following metrics:

- TTC at the AEB trigger time
- Trigger time difference
- Crash avoidance rate and injury risk reduction
- Speed reduction of all cases and speed of the remaining crashes
- Impact location of the remaining crashes

Two metrics related to the AEB trigger time were analysed: the TTC at trigger time and the difference in trigger times between each CAEB and the TAEB. TTC is calculated here as the time duration from when the AEB triggers to when the car reaches the predicted collision point. The TTC is not only

an indicator of situation criticality—it is also sometimes used directly as part of AEB algorithms in virtual simulation studies [19, 20]. Trigger time is an indicator of AEB performance, because, for each individual crash, the earlier the trigger time, the higher the crash avoidance potential. The second metric, trigger time difference, was calculated for the CAEB algorithms by subtracting each CAEB algorithm’s trigger time from that of the TAEB algorithm for each crash. This difference can be interpreted as quantifying how much earlier (negative value) or later (positive value) each CAEB activated compared to the TAEB.

While trigger time differences provide a clear comparison for the different AEBs’ activation times, crash avoidance rate and injury risk reduction are the main direct metrics for evaluating and comparing their safety impact. For each algorithm, the proportion of avoided crashes was calculated by dividing the number of avoided crashes by the total number of original crashes. The injury risks were calculated using three motorcyclist injury risk curves from Ding et al. [52]: at least moderate (MAIS2+), at least serious (MAIS3+), and fatal. (See Gennarelli and Wodzin’s [53] description of MAIS coding for more information.) Details of the injury risk curves can be found in Appendix E.

Two speed-related metrics are also analysed: the remaining crashes’ impact speed (the speed of the car with AEB when the crash was not avoided) and the speed reduction (the impact speed of the car with AEB subtracted from the original

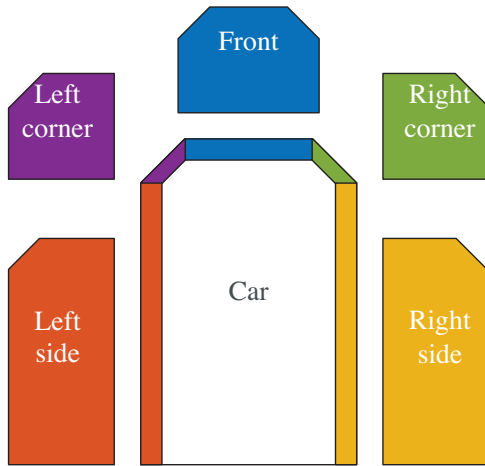


FIGURE 3 Illustration of car impact locations of remaining crashes.

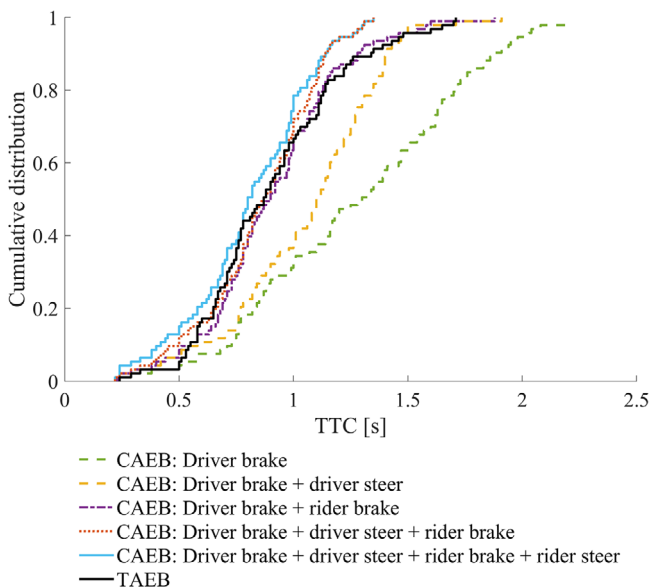


FIGURE 4 Cumulative distribution of TTC at the AEB trigger time for the TAEB and the five CAEBs.

impact speed). Both metrics are presented as cumulative distributions to provide graphical comparisons of the algorithms' performances.

Car impact location is an important metric when developing in-crash safety systems. The impact locations for the remaining crashes are divided into five areas: front, left corner, right corner, left side, and right side (see Figure 3).

3 | RESULTS

3.1 | TTC and trigger time

Two time plots are presented: the plot of the TTC at the AEB trigger time (Figure 4) and the trigger time differences between each CAEB and the TAEB (Figure 5). In Figure 4, CAEB:

'Driver brake' has the highest TTC cumulative distribution (with a 50th percentile of 1.3 s). When the options 'driver steer', 'rider brake', and/or 'rider steer' are added in the CAEB algorithm, the TTC at trigger time tends to decrease, with a 50th percentile of 0.8 s when all four avoidance options are included. Note that for the cumulative distributions, the individual original cases may have different TTCs, depending on the algorithm (e.g. is they are not 'matched' by case on any axis). In general, the TTC at the CAEB trigger time is decreasing as the number of avoidance manoeuvre options increases. This is particularly evident for the CAEB algorithms with the lowest number of avoidance manoeuvre options ('CAEB: Driver brake', and 'CAEB: Driver brake + driver steer'), while the algorithms with a higher number of avoidance manoeuvre options have TTC distributions closer together (although it is clear that the algorithm with the higher number of comfortable avoidance option has the lowest TTCs).

Figure 5 offers a more direct comparison between each CAEB and the TAEB by illustrating the trigger time differences. The algorithm CAEB: 'Driver brake' naturally always triggers before or at the same time as the TAEB, because the vehicle's braking limit is well beyond that of the driver's comfort zone. The other four CAEB simulations triggered the AEB braking intervention before the TAEB in some cases, and after the TAEB in others (shown as negative times and positive times in Figure 5, respectively). The safety benefit of triggering at the point of driver discomfort (at the CZB)—when it is earlier than the point of no return—is obvious. In line with what Figure 4 shows, Figure 5 shows that as more options of comfortable avoidance (when the road users can brake or steer comfortably to avoid the crash) are included in the algorithm, the CAEB triggers later. It must be noted that, although likely reducing nuisance interventions, a CAEB triggering later than the TAEB (positive values in Figure 5) will lead to more critical situations—and, possibly, to worse performance—compared to the TAEB.

3.2 | Crash avoidance and injury risk reduction

Naturally, all the CAEB algorithm variants that can never trigger later than the TAEB algorithm show better performance than the TAEB algorithm. As shown in Table 4, when the CAEB algorithms are allowed to trigger later than TAEB (aiming to reduce the number of false positives by considering comfortable manoeuvres), the CAEB: 'Driver brake' shows substantially better performance than the other five algorithms. Three algorithms (TAEB, CAEB: 'Driver brake + driver steer + rider brake + rider steer', and CAEB: 'Driver brake + driver steer + rider brake') had similar proportions of avoided crashes. Because the CAEBs with more comfortable avoidance manoeuvres were less effective at reducing impact speed, their effectiveness in terms of both crash avoidance and injury risk reduction was concomitantly reduced. The proportion of avoided crashes ranged from approximately 44%, when all four CZBs (driver and rider braking and steering) were considered, to over 80% when only comfortable driver braking was

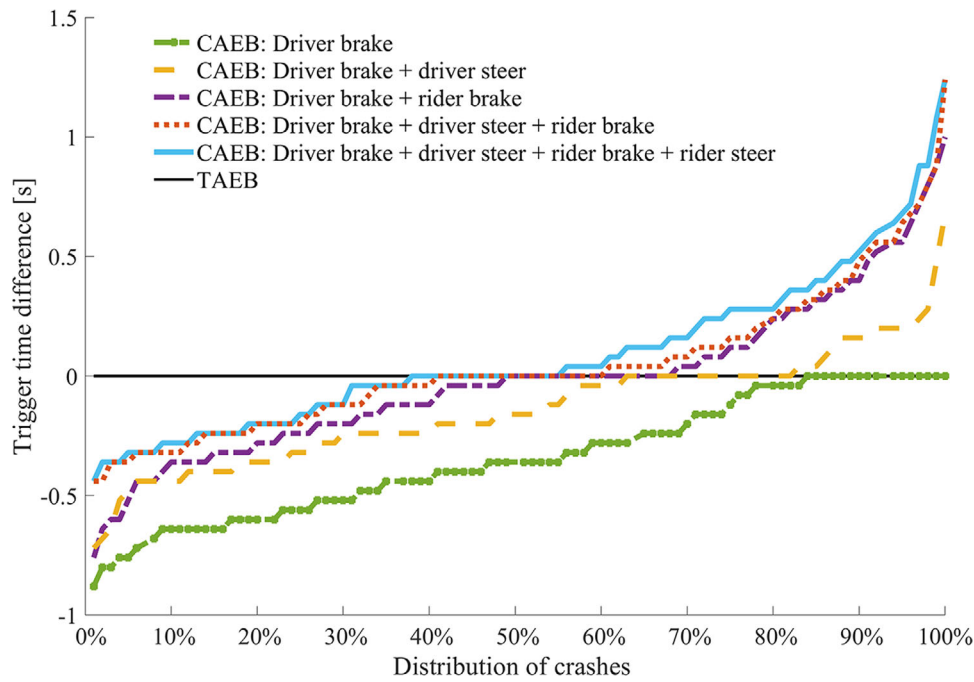


FIGURE 5 Comparison of AEB trigger time differences. The horizontal black line at zero is the trigger time of the TAEB. The other lines represent the trigger time differences between each of the five CAEB algorithms and the TAEB algorithm. The 93 simulated crashes, represented by 0–100% on the *x*-axis, are ordered from left to right by increasing trigger time difference, independently for each algorithm.

TABLE 4 For each AEB, percent crash avoidance and percent injury risk reduction (for all original crashes and remaining crashes, respectively) are given; the injury reduction results include the mean injury risk reduction in MAIS2+, MAIS3+, and fatal injuries. In addition, the crash avoidance results for the algorithm variants (which only consider the CAEB when it triggers earlier than the TAEB) are also shown.

Algorithms	Crash avoidance	Crash avoidance (no later than TAEB)	Injury risk reduction					
			All crashes			Remaining crashes		
			MAIS2+	MAIS3+	Fatal	MAIS2+	MAIS3+	Fatal
CAEB: Driver brake	83.9%	83.9%	88.0%	88.5%	90.4%	25.5%	29.0%	40.4%
CAEB: Driver brake + driver steer	66.7%	72.0%	75.5%	76.4%	79.4%	26.5%	29.1%	38.3%
CAEB: Driver brake + rider brake	53.8%	65.6%	64.9%	66.0%	70.8%	24.1%	26.4%	36.8%
CAEB: Driver brake + driver steer + rider brake	46.2%	60.2%	59.4%	60.6%	66.3%	24.8%	27.0%	37.5%
CAEB: Driver brake + driver steer + rider brake + rider steer	44.1%	60.2%	58.8%	59.8%	64.9%	23.3%	25.3%	34.7%
TAEB	48.4%	48.4%	62.2%	62.9%	65.6%	26.7%	28.1%	33.4%

considered. As expected (and conceptually demonstrated in Figure 1), when more options are added to the CAEB, the system’s performance is reduced, since the algorithms with more comfortable avoidance options must ‘pass’ more algorithmic thresholds to trigger the vehicle’s emergency braking.

3.3 | Impact speed reduction, impact speed, and location

The algorithms were compared with respect to impact speed reduction (for all 93 original crashes) and the impact speed

of the remaining crashes (left and right plots, respectively, in Figure 6). The reduction in impact speed was calculated for each AEB by subtracting the speed of the simulated impact (with AEB) from the original impact speed. (When a crash was avoided with the CAEB, the impact speed of the simulation was set to zero, resulting in a speed reduction in Figure 6, left, equal to the impact speed of the original crash.) The CAEB: ‘Driver brake’ reduced speed more than the other four CAEBs (and the TAEB), since it is the only CAEB with just one comfortable manoeuvre.

Overall, the impact speeds for the remaining crashes are relatively similar across the CAEB algorithms, while those for

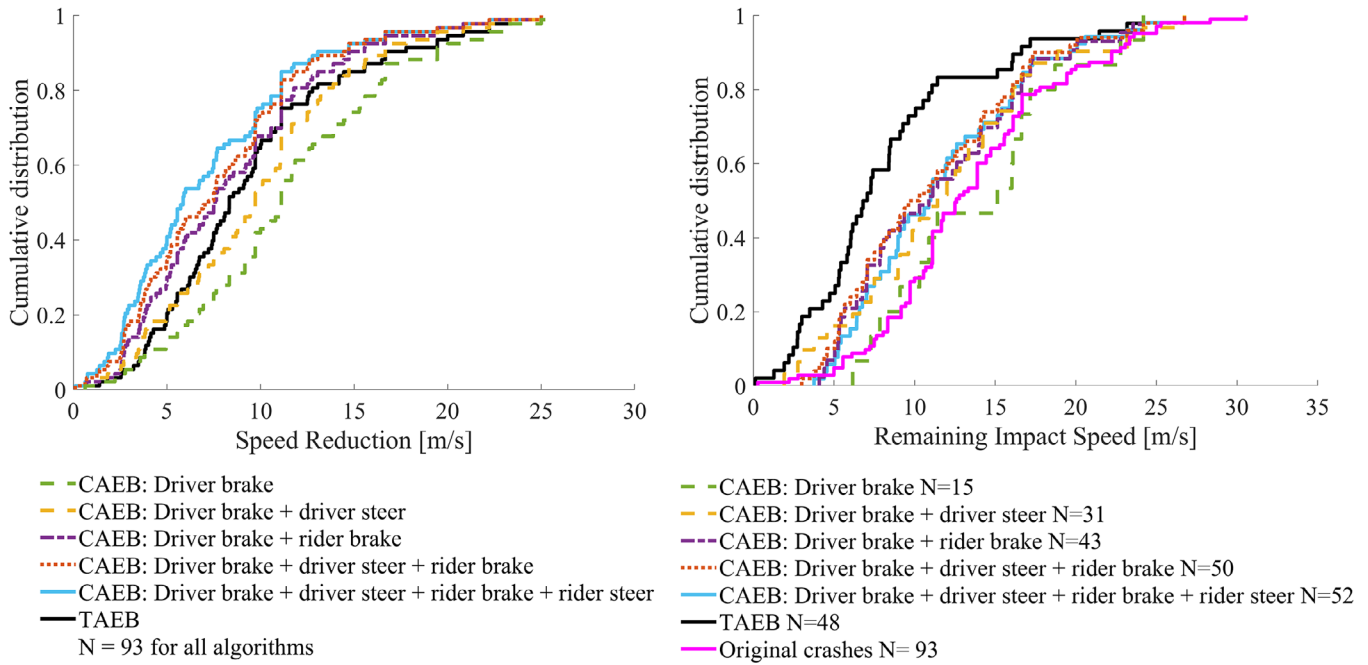


FIGURE 6 Cumulative distribution plots. Left: the speed reductions in all original crashes after the application of the six AEBs. Right: impact speed in remaining crashes. N is the number of crashes; in the right panel it is different for each algorithm, as each avoids a different number of crashes.

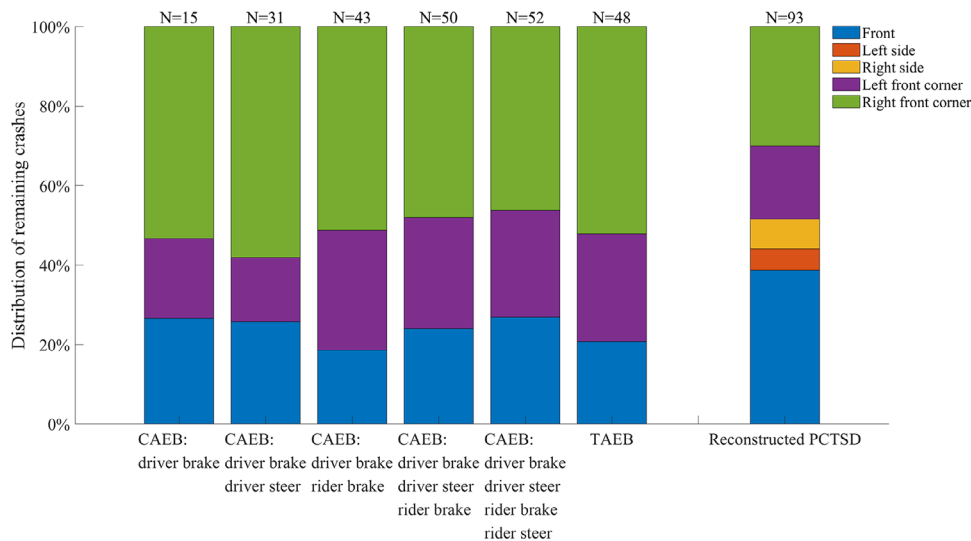


FIGURE 7 Overall distribution of impact locations of reconstructed PCTSD (far right) and remaining crashes for each AEB algorithm. N = number of remaining crashes for that algorithm (i.e. the number of crashes that still occurred when the algorithm was applied to the set of 93 crashes).

TAEB are lower. Note that, to some extent, the crashes avoided by the TAEB had lower original impact speeds. This difference accounts for the lower remaining crash impact speeds for TAEB.

It is noteworthy that all six AEB algorithms have similar overall distributions for the impact locations of the remaining crashes (Figure 7), while the impact locations of the reconstructed PCTSD crashes are quite different. The AEB algorithm distributions have fewer front crashes, more right corner crashes, and no side crashes.

4 | DISCUSSION

In this study we investigated the performance of six different PTW-AEB algorithms, five of which utilized a variety of CZB-based components, by virtually applying the algorithms to 93 reconstructed Chinese car-to-PTW crashes. For each of the AEB algorithms, we also compared the original crash characteristics to the characteristics of the crashes that remained after the (virtual) AEB application. As PTW-AEB algorithms evolve, identifying future remaining crash characteristics can help the

automotive industry develop appropriate in-crash protection systems.

4.1 | Performance of the algorithms

The earlier a car's AEB activates, the more time it has to reduce the car's speed, avoiding some crashes and mitigating injuries in those that occur: Figure 5 confirms earlier findings by Hamdane et al. [54] and Rosén [15]. However, as the information about each manufacturer's algorithm is proprietary [13], the specific details responsible for the timing of an algorithm's activation are typically not available. Although the six included algorithms may not correspond exactly to those in current or future cars, we believe that the range of algorithms (and the relatively large spread in trigger times) provides a reasonable basis for understanding what crash scenarios might (and might not) be avoided by future PTW-AEB systems. Future in-crash protection systems should target the remaining crashes.

Brake activation of the CAEB algorithms can occur earlier or later than that of TAEB, depending on the individual crash configuration. Figure 4 shows that the performance is no worse than TAEB for 55–80% of the crashes, depending on the version of CAEB. Triggering earlier may not always be necessary, but it adds to the safety margin, which may be critically important when braking performance has been reduced. Factors which affect braking, such as road friction, are not included in the TAEB algorithm—and are not usually known by the AEB in real traffic. If future PTW-AEBs only consider drivers' braking and steering CZBs, performance is not unreasonably affected. It should be noted that despite the performance reduction of CAEBs in some cases due to later triggering, the overall performance of the CAEB algorithm which considers driver braking only is substantially better (Figure 4; 83.9% avoidance) than both the TAEB in this study (48.4% avoidance) and the PTW-AEB in Sui et al. [20] (maximum estimated avoidance of 60% with a TTC-based AEB). The 50th percentiles of TTC at trigger time of the proposed CAEBs range from 0.8 to 1.3 s, similar to what Saadé et al. [19] and Sui et al. [20] used in their PTW-AEB assessments (1.0 and 1.1 s, respectively). That is, the CAEB's 50th percentile is close to what others have used as PTW-AEB trigger times, but the CZB component generates interventions both earlier (likely resulting in improved crash avoidance in case of low road friction, for example) and later (avoiding false positives when the driver still feels comfortable and an intervention is not desired).

It is obvious that an AEB relying on TTC alone to trigger does not account for the complexities of daily driving situations and potentially results in unnecessary AEB activations. For this reason, required-deceleration-based triggers like the TAEB have been proposed (by, for example, Brännström et al. [36]). However, these triggers only consider the physical limits of the vehicle, not the driver's perception of comfort—as our proposed CAEB algorithms do.

Our results show that including some sort of CAEB in future AEB designs is likely to enhance their safety performance. If the CAEB is designed to never trigger later than TAEB, an

increased crash avoidance performance of CAEB over TAEB can be guaranteed (as shown in Table 4)—perhaps at the cost of a few more nuisance activations. Including CZB components in AEB algorithms may be particularly advantageous for difficult scenarios, in which current AEB systems sometimes trigger too late or not at all [55, 56]. For pedestrian-AEB systems, AAA [55] has demonstrated that difficult scenarios include those involving child pedestrians, groups of pedestrians, and encounters with pedestrians after curves; for cyclist-AEB systems, TCH [56] shows that scenarios that involve stationary cyclists and cars encountering cyclists in curves are challenging. Although we cannot explicitly demonstrate that CAEB will improve the performance in these specific situations, the more robust activation that it provides in many cases should be beneficial, while avoiding false-positive activations [29, 57, 58]. As CAEBs are designed based on road users' CZBs and the TAEB only considers the vehicle's physical limit of deceleration, it could happen that the TAEB triggers when the driver still has options to avoid the crash comfortably by themselves, leading to more false-positive activations. This, in turn, may result in the driver getting annoyed with the system, which may, in itself, result in discomfort and that the driver disables the system (in the case of AEB that may not be possible, but for other safety systems, such as forward collision warning systems, this may be the case). The false-positive rates of PTW-AEBs in the real world are still to be evaluated. It is thus unclear if there is a need to delay the intervention beyond the TAEB (see Figure 4). If there is no such need, and the algorithm were designed to never brake later than TAEB, it would still reap the benefit of CAEB's earlier triggers—so the performance would always be better than that of TAEB, and likely to substantially improve PTW-AEB performance compared to traditional AEB algorithms. It is worth noting that if only the drivers' CZB options are included in the AEB (and not the PTW riders'), then the current CAEB implementation can be used as is for interactions with cyclists. In order for AEBs to include cyclist's CZB (or, rather the drivers 'idea' of the rider's CZB), those boundaries need to be quantified in future studies. The use of CAEB for pedestrian-AEB would be more complicated, as pedestrians' direction of motion is less predictable than that of cyclists.

4.2 | The implications of remaining-crash characteristics for in-crash protection system development

In this study we found that the remaining crashes for the six AEB variants occur at high speeds. For example, the maximum impact speed of the remaining crashes with the CAEB: 'Driver brake + rider brake' was still 24.2 m/s (median of about 10.3 m/s). At these speeds, injuries are likely. It is, however, possible to decrease injury risks in crashes, as well-established pedestrian protections show. Pedestrian protection offered by passenger cars is tested at 11.1 m/s in Euro NCAP [59], with many cars receiving excellent scores. These scores correlate well with real-world injury reductions, as Strandroth et al. have demonstrated [60].

We also found that, for all AEB variations, the remaining crashes have similar distributions of car impact locations (see Figure 7): mainly the front, right front corner, and left front corner. The distributions are consistent with those reported for the car-to-pedestrian [61] and car-to-bicyclist [62] crashes that occurred with AEB-equipped cars. PTW impacts with vehicle corners have a higher probability of the PTW rider's head impacting the car's A-pillars than, for example, the front of the vehicle. Because A-pillars are particularly stiff, the impact is likely to cause a head injury. An external airbag covering vehicle A-pillars could soften the impact, offering substantial benefits in car-to-PTW crashes—comparable to the benefits identified in car-to-pedestrian [63] and car-to-bicycle crashes [64]. Since all the algorithms had similar impact location distributions, the system design likely does not need to be tuned to the specific AEB and can therefore be generic (and thus cost-efficient).

In addition to in-vehicle protective systems, protective equipment for riders, such as helmets [65] and energy-absorbing and -distributing clothing [66], can also improve rider safety. The protection is fairly independent of the impact location. However, protection at high speeds is limited [67, 68]. Importantly, however, the benefits of these protective systems can increase substantially with only a moderate reduction in impact speed, which PTW-AEB may provide.

4.3 | Limitations and future work

The relatively low number of crashes (93) is one limitation of this study. However, there are few, if any, Chinese databases that include the type (and even amount) of reconstructed car-to-PTW data that we used in this study. Consequently, we have worked with what is available, and we believe that the overall conclusions still hold. Results from the algorithms' applications to the nine crash scenarios (resulting from the categorization of the 93 original crashes) can be found in Appendix A, but we did not find any obvious substantial differences in the algorithms' performances in the different scenarios. Future work might help to understand the differences in more detail. For example, we recommend that future studies investigate if the results would be similar if they were applied to other databases, even data from other countries (such as the GIDAS data in German), as a way to corroborate our findings.

In our calculations, we considered all sensors to be ideal (perfectly accurate and functioning at all times), and we used a large sensor field of view, as we do not know what future systems will use (see Appendix B for details of the selection). Further, the vehicle dynamics were simplified, and we modelled brake interventions by applying direct acceleration (rather than applying brake pedal pressure, for example). Results from the simulations may not be highly accurate with respect to absolute effectiveness estimates; however, even more advanced simulation frameworks are typically not perfect and often overestimate true performance [47].

The CAEB algorithms are based on the concept that the car drivers' comfort zone boundaries apply not only to their own car but also to the drivers' assumptions about the PTW

riders (what the drivers expect the riders to do in everyday riding situations). This simplification was made in part due to the fact that, while we were able to draw on previous literature quantifying the CZBs of drivers with respect to lateral and longitudinal acceleration [33, 34], we did not find any convincing literature on the CZBs for PTW riders' braking and steering. More work is needed to quantify PTW riders' CZBs with respect to lateral and longitudinal acceleration. However, it is the driver's perception that is important when applying CZBs in in-car AEB algorithms, because it is the false-positive AEB interventions that are being targeted. (Note that Cicchino [69] has studied the comfort of drivers in interactions with pedestrians, but without quantifying comfort in terms of kinematics.) Consequently, we believe that our use of car CZBs for PTWs is a reasonable preliminary approach. It is expected that better data will reveal that car and PTW CZBs (both those of the PTW riders themselves and those that the car drivers think are the PTW riders') are likely to be more similar for braking than for steering, due to PTWs' greater instability and agility. Future research should also include sensitivity analyses on the impact of the choice of CZBs on the safety benefit assessment results. It should also be noted that AEB algorithm designers who consider comfort-based algorithms will have to verify the acceptance of the specific implementations, especially if the actual comfort zones according to PTW riders are also included in the algorithm.

An assessment of false-positive activations is beyond the scope of the study; we did not have access to the data that would make such an assessment possible. Ideally, this assessment should be included in future studies—by applying the AEB algorithms to everyday driving data or near-crash situations and quantifying how often the different AEB algorithms trigger an intervention that is not warranted.

In the future, the algorithm variations applied to car-to-PTW data from China in this study could be applied to car-to-PTW crash data from other countries, thereby providing country-specific information about system design and market planning to safety system suppliers. The variations should also be assessed as part of automated vehicle crash prevention functionality for higher levels of automation [70].

5 | CONCLUSIONS

Using pre-crash kinematics data from the Chinese in-depth database SHUFO, we have estimated the characteristics of the remaining crashes while assessing the potential safety benefits of six different AEB algorithms for cars encountering PTWs. Our main findings are that the impact speed and impact locations for the remaining crashes are similar across algorithms, and that no matter which AEB algorithm is employed, it is likely that there will be a substantial number of crashes remaining with high impact speeds—which will require effective in-crash protective systems. Although impact speed and location are important variables for in-crash protection systems, the finding that they were not substantially influenced by the various AEB algorithms indicates that the design and development of these systems can

be relatively generic. This simplification may make the systems more affordable, enabling greater market penetration and thus saving more lives.

Another key finding is that including drivers' or riders' comfortable manoeuvres in the PTW-AEB algorithm enables braking earlier in many situations, while likely keeping the number of nuisance interventions to a minimum. When only the driver's CZBs are considered in the algorithms, the average safety performance is higher than that of the traditional required-deceleration algorithm, even allowing for a delay in activation for some crash events. If an AEB algorithm considers CZB-based interventions only when they occur earlier than the interventions of more traditional algorithms (e.g. based on required decelerations, which never trigger later than the point of no return), then including a CZB-based algorithm will always avoid more crashes and reduce more injuries than the traditional algorithms. If CZB-based PTW-AEB algorithms are adopted by the automotive industry, the number of people dying or getting injured in car-to-PTW crashes is likely to decrease.

AUTHOR CONTRIBUTIONS

Xiaomi Yang: Conceptualization; data curation; formal analysis; methodology; software; writing—original draft. **Nils Lubbe:** Conceptualization; funding acquisition; methodology; supervision; writing—review & editing. **Jonas Bärgrman:** Conceptualization; funding acquisition; methodology; supervision; writing—review & editing.

ACKNOWLEDGEMENTS

First and foremost, the authors would like to thank Autoliv Development AB, who provided funding to start this work. The authors would like to thank Yutong He from SHUFO for his support, including explaining the SHUFO data. Further, the authors highly appreciate the support from Autoliv employees Hanna Jeppsson, Bo Sui, and Junaid Shaikh on the reconstruction and interpretation of the in-depth crash databases, as well as Erik Rosén for developing the simulation framework used as a basis for this study. The authors would like to thank András Bálint from Chalmers University of Technology for his valuable suggestions in interpreting the results from a statistical point of view. The authors also thank the European Commission, since the finalization of simulations, the analysis, and much of the paper writing and revision was funded by the SHAPE-IT project under the European Union's Horizon 2020 research and innovation programme (under the Marie Skłodowska-Curie grant agreement 860410). Finally, The authors also want to thank Kristina Mayberry (Mayberry Academic Services) for her language review.

CONFLICT OF INTEREST STATEMENT

Nils Lubbe works at Autoliv Research, located in Vårgårda, Sweden. Autoliv Research is part of Autoliv (www.autoliv.com), a company that develops, manufactures and sells for example protective safety systems to car manufacturers. Results from this study may impact how Autoliv choose to develop their products.

DATA AVAILABILITY STATEMENT

The data that support the findings of this study are available at Autoliv Research. Restrictions apply to the availability of these data, as the original cases (based on which the crash reconstructions were made) were under license for use in this study. Data availability from Autoliv may also be restricted by the data provider SHUFO.

ORCID

Xiaomi Yang  <https://orcid.org/0000-0003-1641-9634>

REFERENCES

- World Health Organization, Global status report on road safety: The Southeast Asia story. https://www.unescap.org/sites/default/files/RoadSafetyDataManagement-WHOGlobalStatusReportonRoadSafety-WHO_0.pdf (2019)
- World Health Organization, Powered two- and three-wheeler safety: a road safety manual for decision-makers and practitioners. <https://www.who.int/publications/i/item/9789240060562> (2022)
- National Bureau of Statistics of China, China statistical yearbook: basic statistics on traffic accidents. <https://www.stats.gov.cn/sj/ndsj/2023/indexeh.htm> (2023). Accessed 20 Mar 2024
- Isaksson-Hellman, I., Norin, H.: How thirty years of focused safety development has influenced injury outcome in Volvo cars. *Annu. Proc. Assoc. Adv. Automot. Med.* 49, 63–77 (2005)
- Tay, Y.Y., Lim, C.S., Lankarani, H.M.: A finite element analysis of high-energy absorption cellular materials in enhancing passive safety of road vehicles in side-impact accidents. *Int. J. Crashworthiness* 19, 288–300 (2014). <https://doi.org/10.1080/13588265.2014.893789>
- Jarašūniene, A., Jakubauskas, G.: Improvement of road safety using passive and active intelligent vehicle safety systems. *Transport* 22, 284–289 (2010). <https://doi.org/10.1080/16484142.2007.9638143>
- Li, J., Ao, D.: Subjective assessment for an advanced driver assistance system: a case study in China. *J. Intell. Connected Veh.* 5, 112–122 (2022). <https://doi.org/10.1108/JICV-11-2021-0017>
- Zhang, Y., Li, J., Liu, X.: Research on integrated navigation in AEB system based on multi-source fusion. In: *IET Conference Proceedings*, pp. 37–42. IET, London (2020)
- Chelbi, N.E., Gingras, D., Sauvageau, C.: Proposal of a new virtual evaluation approach of preventive safety applications and advanced driver assistance functions—application: AEB system. *IET Intell. Transp. Syst.* 12, 1148–1156 (2018). <https://doi.org/10.1049/iet-its.2018.5269>
- Cicchino, J.B.: Effectiveness of forward collision warning and autonomous emergency braking systems in reducing front-to-rear crash rates. *Accid. Anal. Prev.* 99, 142–152 (2017). <https://doi.org/10.1016/j.aap.2016.11.009>
- Fildes, B., Keall, M., Bos, N., Lie, A., Page, Y., Pastor, C., Pennisi, L., Rizzi, M., Thomas, P., Tingvall, C.: Effectiveness of low speed autonomous emergency braking in real-world rear-end crashes. *Accid. Anal. Prev.* 81, 24–29 (2015). <https://doi.org/10.1016/j.aap.2015.03.029>
- Jeppsson, H., Östling, M., Lubbe, N.: Real life safety benefits of increasing brake deceleration in car-to-pedestrian accidents: simulation of vacuum emergency braking. *Accid. Anal. Prev.* 111, 311–320 (2018). <https://doi.org/10.1016/j.aap.2017.12.001>
- Haus, S.H., Sherony, R., Gabler, H.C.: Estimated benefit of automated emergency braking systems for vehicle – pedestrian crashes in the United States. *Traffic Inj. Prev.* 20, S171–S176 (2019). <https://doi.org/10.1080/15389588.2019.1602729>
- Chajmowicz, H., Saadé, J., Cuny, S., Rosén, E., Zhao, Y., Ito, D., Mizuno, K., Chajmowicz, H., Saadé, J., Cuny, S., Rizzi, M.M.C., Rizzi, M.M.C., Kullgren, A., Algurén, B.: Prospective assessment of the effectiveness of autonomous emergency braking in car-to-cyclist accidents in France. *Traffic Inj. Prev.* 21, 215–221 (2019). <https://doi.org/10.1080/15389588.2020.1730827>

15. Rosén, E.: Autonomous emergency braking for vulnerable road users. In: 2013 IRCOBI Conference Proceedings—International Research Council on the Biomechanics of Injury, pp. 618–627. IRCOBI, Farmington Hills, MI (2013)
16. Zhao, Y., Ito, D., Mizuno, K.: AEB effectiveness evaluation based on car-to-cyclist accident reconstructions using video of drive recorder. *Traffic Inj. Prev.* 20, 100–106 (2019). <https://doi.org/10.1080/15389588.2018.1533247>
17. Zhao, M., Wang, H., Chen, J., Xu, X., He, Y.: Method to optimize key parameters and effectiveness evaluation of the AEB system based on rear-end collision accidents. *SAE Int. J. Passeng. Cars Electron. Electr. Syst.* 10, 310–317 (2017). <https://doi.org/10.4271/2017-01-0112>
18. Dean, M.E., Haus, S.H., Sherony, R., Gabler, H.C.: Potential crash benefits of motorcycle-detecting automatic emergency braking systems. In: IRCOBI (International Research Council On the Biomechanics of Impact) Conference, pp. 39–50. IRCOBI, Farmington Hills, MI (2021)
19. Saadé, J., Chajmowicz, H., Cuny, S.: Prospective evaluation of autonomous emergency braking systems performance in car-to-powered two-wheelers accidents in France. In: IRCOBI (International Research Council On the Biomechanics of Impact) Conference, pp. 97–108. IRCOBI, Farmington Hills, MI (2022)
20. Sui, B., Lubbe, N., Bärgrman, J.: Evaluating automated emergency braking performance in simulated car-to-two-wheeler crashes in China: a comparison between C-NCAP tests and in-depth crash data. *Accid. Anal. Prev.* 159, 106229 (2021). <https://doi.org/10.1016/j.aap.2021.106229>
21. guo Zhao, Z., jia Zheng, X., qiang Wang, J., Xu, Q., Kodaka, K.: Assessing performance of collision mitigation brake system in Chinese traffic environment. *J. Cent. South Univ.* 26, 2854–2869 (2019). <https://doi.org/10.1007/s11771-019-4219-z>
22. Najm, W.G., Mironer, M.S., Fraser, L.C.: Analysis of target crashes and ITS/countermeasure actions, intelligent transportation: serving the user through deployment. In: Proceedings of the 1995 Annual Meeting of ITS America, pp. 931–940. ITS America, Washington, D.C. (1995)
23. Rixinger, L.E., Sherony, R., Gabler, H.C.: Residual road departure crashes after full deployment of LDW and LDP systems. *Traffic Inj. Prev.* 20, S177–S181 (2019). <https://doi.org/10.1080/15389588.2019.1603375>
24. Östling, M., Jeppsson, H., Lubbe, N.: Predicting crash configurations in passenger car to passenger car crashes to guide the development of future passenger car safety. In: IRCOBI Conference Proceedings International Research Council on the Biomechanics of Injury, pp. 626–643. IRCOBI, Farmington Hills, MI (2019)
25. Euro NCAP: Euro NCAP Rating Review 2018: Report from the Ratings Group. <https://cdn.euroncap.com/media/41777/ratings-group-report-2018-version-11-with-appendices.201811121629591429.pdf> (2018). Accessed 6 Jul 2024
26. Diederichs, F., Schuttke, T., Spath, D.: Driver intention algorithm for pedestrian protection and automated emergency braking systems. In: IEEE Conference on Intelligent Transportation Systems, Proceedings, ITSC, pp. 1049–1054. IEEE, Piscataway, NJ (2015)
27. Scanlon, J.M., Sherony, R., Gabler, H.C.: Injury mitigation estimates for an intersection driver assistance system in straight crossing path crashes in the United States. *Traffic Inj. Prev.* 18, S9–S17 (2017). <https://doi.org/10.1080/15389588.2017.1300257>
28. Sander, U.: Opportunities and limitations for intersection collision intervention—a study of real world ‘left turn across path’ accidents. *Accid. Anal. Prev.* 99, 342–355 (2017). <https://doi.org/10.1016/j.aap.2016.12.011>
29. Källhammer, J.-E.: Using false alarms when developing automotive active safety systems. Dissertation, Linköping University (2011)
30. Lees, M.N., Lee, J.D.: Enhancing safety by augmenting information acquisition in the driving environment, human factors of visual and cognitive performance in driving. In: Human Factors of Visual and Cognitive Performance in Driving, pp. 167–186. Taylor & Francis, Milton Park (2009)
31. Summala, H.: Towards understanding motivational and emotional factors in driver behaviour: comfort through satisficing. In: Cacciabue, P.C., (Ed.) *Modelling Driver Behaviour in Automotive Environments*, pp. 189–207. Springer, Berlin, Heidelberg (2007)
32. Ljung Aust, M., Dombrovski, S.: Understanding and improving driver compliance with safety system. Paper presented at the 23th international technical conference on the enhanced safety of vehicles (ESV), Seoul, 27 May 2013
33. Kiefer, R.J., Cassar, M.T., Flannagan, C.A., LeBlanc, D.J., Palmer, M.D., Deering, R.K., Shulman, M.A.: Forward Collision Warning Requirements Project: Refining the CAMP Crash Alert Timing Approach by Examining “Last-Second” Braking and Lane Change Maneuvers Under Various Kinematic Conditions. National Highway Traffic Safety Administration, Berlin (2003)
34. Bärgrman, J., Smith, K., Werneke, J.: Quantifying drivers’ comfort-zone and dread-zone boundaries in left turn across path/opposite direction (LTAP/OD) scenarios. *Transp. Res. Part F: Traffic Psychol. Behav.* 35, 170–184 (2015). <https://doi.org/10.1016/j.trf.2015.10.003>
35. Puthan, P., Lubbe, N., Shaikh, J., Sui, B., Davidsson, J.: Defining crash configurations for powered two-wheelers: comparing ISO 13232 to recent in-depth crash data from Germany, India and China. *Accid. Anal. Prev.* 151, 105957 (2021). <https://doi.org/10.1016/j.aap.2020.105957>
36. Brännström, M., Sjöberg, J., Coelingh, E.: A situation and threat assessment algorithm for a rear-end collision avoidance system. In: IEEE Intelligent Vehicles Symposium, Proceedings, pp. 102–107. IEEE, Piscataway, NJ (2008)
37. Delucia, P.C.R., Jones, K.S.: Gibson and Crooks (1938): vision and validation. *Am. J. Psychol.* 130, 413–429 (2017). <https://doi.org/10.5406/amerjpsyc.130.4.0413>
38. Page, Y., Fahrenkrog, F., Fiorentino, A., Gwehenberger, J., Helmer, T., Lindman, M., Op den Camp, O., van Rooij, L., Puch, S., Fränze, M., Sander, U., Wimmer, P.: A comprehensive and harmonized method for assessing the effectiveness of advance driver assistance systems by virtual simulation. In: The 24th International Technical Conference on the Enhanced Safety of Vehicles (ESV), pp. 1–12. National Highway Traffic Safety Administration, Washington, D.C. (2015)
39. Lindman, M., Tivesten, E.: A method for estimating the benefit of autonomous braking systems using traffic accident data. *SAE Tech. Pap.* 2006-01-0473 (2006). <https://doi.org/10.4271/2006-01-0473>
40. Scanlon, J.M., Kusano, K.D., Daniel, T., Alderson, C., Ogle, A., Victor, T.: Waymo simulated driving behavior in reconstructed fatal crashes within an autonomous vehicle operating domain. *Accid. Anal. Prev.* 163, 106454 (2021). <https://doi.org/10.1016/j.aap.2021.106454>
41. Rosén, E., Källhammer, J.E., Eriksson, D., Nentwich, M., Fredriksson, R., Smith, K.: Pedestrian injury mitigation by autonomous braking. *Accid. Anal. Prev.* 42, 1949–1957 (2010). <https://doi.org/10.1016/j.aap.2010.05.018>
42. Ding, C., Bohman, K., Zhang, W., Li, Y., Zhao, X.: Rear seated occupants in near-side impacts -study based on Chinese accident databases. 13th International Forum of Automotive Traffic Safety (INFATS), pp. 0–5. Hunan University, Changsha (2016)
43. Schubert, A., Liers, H., Petzold, M.: The GIDAS pre-crash-matrix 2016. Innovations for standardized pre-crash-scenarios on the basis of the VUFO simulation model VAST, Berichte Der Bundesanstalt Fuer Strassenwesen. In: *Unterreihe Fahrzeugtechnik, Fachverlag NW, Bremen* (2017)
44. Yang, X.: Characterizing Car to Two-Wheeler Residual crashes in China Application of AEB in Virtual Simulation. Chalmers University of Technology, Gothenburg (2019)
45. Wimmer, P., Düring, M., Chajmowicz, H., Granum, F., King, J., Kolk, H., Op den Camp, O., Scognamiglio, P., Wagner, M.: Toward harmonizing prospective effectiveness assessment for road safety: Comparing tools in standard test case simulations. *Traffic Inj. Prev.* 20, S139–S145 (2019). <https://doi.org/10.1080/15389588.2019.1616086>
46. Xie, G., Chen, Z., Gao, M., Hu, M., Qin, X.: PPF-Det: point-pixel fusion for multi-modal 3D object detection. *IEEE Trans. Intell. Transport. Syst.* 25(6), 5598–5611 (2023)
47. Sander, U.: Predicting safety benefits of automated emergency braking at intersections virtual simulations based on real-world accident data. Doctoral Thesis, Chalmers University of Technology (2018)

48. Brännström, M., Coelingh, E., Sjöberg, J.: Decision-making on when to brake and when to steer to avoid a collision. *Int. J. Veh. Saf.* 7(1), 87–106 (2014). <https://doi.org/10.1504/IJVS.2014.058243>
49. C-NCAP: C-NCAP management regulation 2018. <http://www.c-ncap.org/> (2018). Accessed 6 Jul 2024
50. Costa, L., Perrin, C., Dubois-lounis, M., Serre, T., Costa, L., Perrin, C., Dubois-lounis, M., Serre, T., Nacer, M.: Modeling of the Powered Two-Wheeler dynamic behavior for emergency situations analysis. in: VSDIA 16th International MINI Conference on Vehicle System Dynamics (2019)
51. C-NCAP: C-NCAP management regulation 2021. <http://www.c-ncap.org/> (2020). Accessed 6 Jul 2024
52. Ding, C., Rizzi, M., Strandroth, J., Sander, U., Lubbe, N.: Motorcyclist injury risk as a function of real-life crash speed and other contributing factors. *Accid. Anal. Prev.* 123, 374–386 (2019). <https://doi.org/10.1016/j.aap.2018.12.010>
53. Gennarelli, T.A., Wodzin, E.: AIS 2005: a contemporary injury scale. *Injury* 37, 1083–1091 (2006). <https://doi.org/10.1016/j.injury.2006.07.009>
54. Hamdane, H., Serre, T., Masson, C., Anderson, R., Hamdane, H., Serre, T., Masson, C., Issues, R.A., Masson, C.: Issues and challenges for pedestrian active safety systems based on real world accidents. *Accid. Anal. Prev.* 82, 53–60 (2015). <https://doi.org/10.1016/j.aap.2015.05.014>
55. AAA: Automatic emergency braking with pedestrian detection. <https://www.aaa.com/AAA/common/aar/files/Research-Report-Pedestrian-Detection.pdf> (2019). Accessed 6 Jul 2024
56. TCH: Radar visibility of two-wheelers. <https://www.tcs.ch/de/testberichte-ratgeber/tests/connected-car/radarsichtbarkeit-von-zweiraedern.php> (2018). Accessed 6 Jul 2024
57. Helmer, T.: Development of a Methodology for the Evaluation of Active Safety Using the Example of Preventive Pedestrian Protection. Springer, Cham (2014)
58. Otubushin, A., Gruber, C., Domsch, C., Integrale Sicherheit, B.M.W.: Effektive schutzmöglichkeiten schwächerer verkehrsteilnehmer, integrated safety: effective possibilities to protect vulnerable road users. In: 6th Praxiskonferenz Fußgängerschutz, carhs, Bergisch-Gladbach (2011)
59. Ratingen, V.M., Williams, A., Lie, A., Seeck, A., Castaing, P., Kolke, R., Adriaenssens, G., Miller, A.: The European new car assessment programme: a historical review. *Chin. J. Traumatol.* 19, 63–69 (2016). <https://doi.org/10.1016/j.cjtee.2015.11.016>
60. Strandroth, J., Sternlund, S., Lie, A., Tingvall, C., Rizzi, M., Kullgren, A., Ohlin, M., Fredriksson, R.: Correlation between Euro NCAP pedestrian test results and injury severity in injury crashes with pedestrians and bicyclists in Sweden. *SAE Tech. Pap.* 58, 213–231 (2014). <https://doi.org/10.4271/2014-22-0009>
61. Puthan, P., Östling, M., Jeppsson, H., Lubbe, N.: Passive safety needs for future cars: predicted car occupant fatalities in the USA. In: Proceedings of FISITA World Automotive Congress, FISITA, Hertfordshire (2018)
62. Jeppsson, H., Lubbe, N.: Simulating automated emergency braking with and without Torricelli vacuum emergency braking for cyclists: effect of brake deceleration and sensor field-of-view on accidents, injuries and fatalities. *Accid. Anal. Prev.* 142, 105538 (2020). <https://doi.org/10.1016/j.aap.2020.105538>
63. Fredriksson, R., Rosén, E.: Head injury reduction potential of integrated pedestrian protection systems based on accident and experimental data – benefit of combining passive and active systems. In: IRCOBI (International Research Council On the Biomechanics of Impact) Conference, pp. 603–613, IRCOBI, Berlin (2014)
64. Fredriksson, R., Ranjbar, A., Rosén, E.: Integrated bicyclist protection systems—potential of head injury reduction combining passive and active protection systems. In: The 24th Enhanced Safety Vehicle (ESV) Conference, pp. 15–51. National Highway Traffic Safety Administration, Washington, D.C. (2015)
65. Fernandes, F.A.O., Alves De Sousa, R.J.: Motorcycle helmets—a state of the art review. *Accid. Anal. Prev.* 56, 1–21 (2013). <https://doi.org/10.1016/j.aap.2013.03.011>
66. Wu, D., Hours, M., Ndiaye, A., Coquillat, A., Martin, J.L.: Effectiveness of protective clothing for motorized 2-wheeler riders. *Traffic Inj. Prev.* 20, 196–203 (2019). <https://doi.org/10.1080/15389588.2018.1545090>
67. Meng, S.: Towards improved motorcycle helmet test methods for head impact protection Using experimental and numerical methods. Doctoral Thesis, KTH Royal Institute of Technology (2019)
68. Ballester, O.C., Llari, M., Honoré, V., Masson, C., Arnoux, P.: An evaluation methodology for motorcyclists' wearable airbag protectors based on finite element simulations. *Int. J. Crashworthiness* 26, 99–108 (2019). <https://doi.org/10.1080/13588265.2019.1687218>
69. Cicchino, J.B.: Effects of automatic emergency braking systems on pedestrian crash risk. *Accid. Anal. Prev.* 172, 106686 (2022). <https://doi.org/10.1016/j.aap.2022.106686>
70. Shuttleworth, J.: SAE Standards News: J3016 automated-driving graphic update. <https://www.sae.org/news/2019/01/sae-updates-j3016-automated-driving-graphic> (2020). Accessed 6 Jul 2024
71. Uittenbogaard, J., den Camp, O.O., van Montfort, S.: CATS Deliverable 5.1: CATS verification of test matrix and protocol. <https://resolver.tno.nl/uuid:145f4830-8d1a-433e-b1ce-0a902ee59938> (2016). Accessed 6 Jul 2024
72. Char, F., Serre, T.: Analysis of pre-crash characteristics of passenger car to cyclist accidents for the development of advanced drivers assistance systems. *Accid. Anal. Prev.* 136, 105408 (2020). <https://doi.org/10.1016/j.aap.2019.105408>

How to cite this article: Yang, X., Lubbe, N., Bärghman, J.: Evaluation of comfort zone boundary based automated emergency braking algorithms for car-to-powered-two-wheeler crashes in China. *IET Intell. Transp. Syst.* 1–17 (2024). <https://doi.org/10.1049/itr2.12532>

APPENDIX A SCENARIO CATEGORIZATION

In the main manuscript of this paper, we have reported only the aggregated results of the application of the algorithms on all 93 SHUFO crashes. In this section we report the results after dividing them into different scenarios, according to the heading directions of the passenger car and the PTW (same categorization as in [44], which in turn is based on [17]): going straight, turning left, or turning right. The going-straight scenarios were further broken down by heading angles and velocities of both vehicles into four scenarios: ‘Straight crossing’ (perpendicular), ‘Straight front-to-front’, ‘Straight, PTW still’, and ‘Rear end’ (car striking moving PTW). There were only two cases in which both the car and the PTW turned—‘Car turns right, PTW turns left’ and ‘Car turns left, PTW turns right’—so they were grouped together into a ‘Both turning’ scenario. Four additional scenarios were defined when one vehicle turned (either left or right) while the other went straight. Figure A1 shows how the cases were distributed across the nine scenarios. ‘Straight crossing’ and ‘Car straight, PTW turns left’ stand out as most prevalent. Note, however, that due to the low number of crashes in some categories, the results should be interpreted with great care.

Categorized scenarios are illustrated in Table A1.

The six AEB algorithms displayed different crash avoidance performances in different scenarios. Figure A2 shows the percent of original crashes for each scenario, as well as

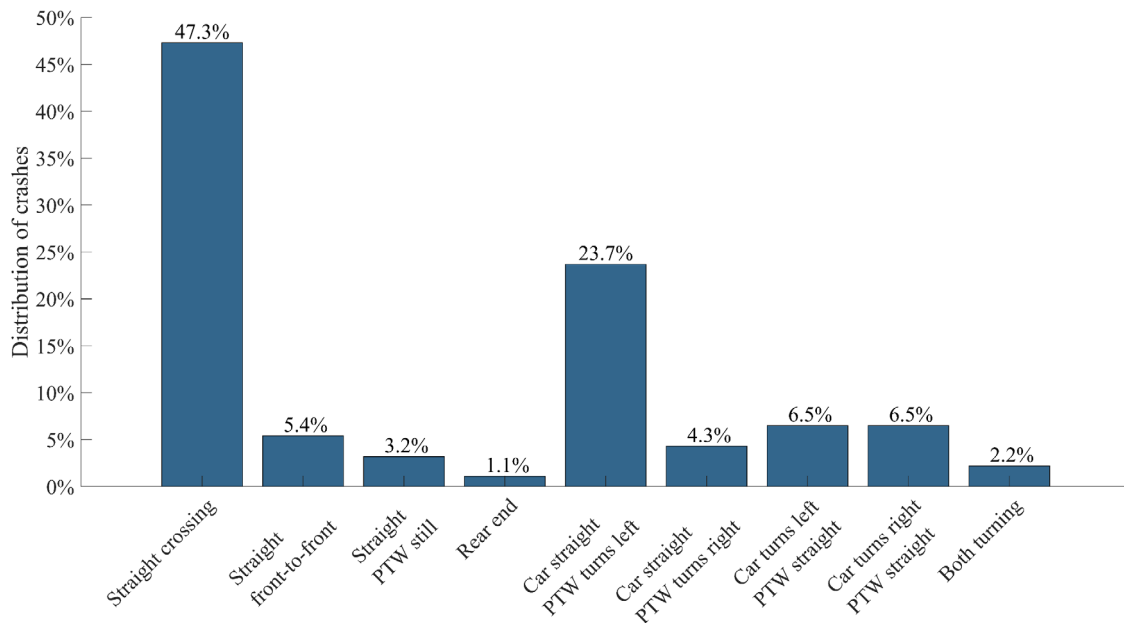


FIGURE A1 Distribution of crash scenarios.

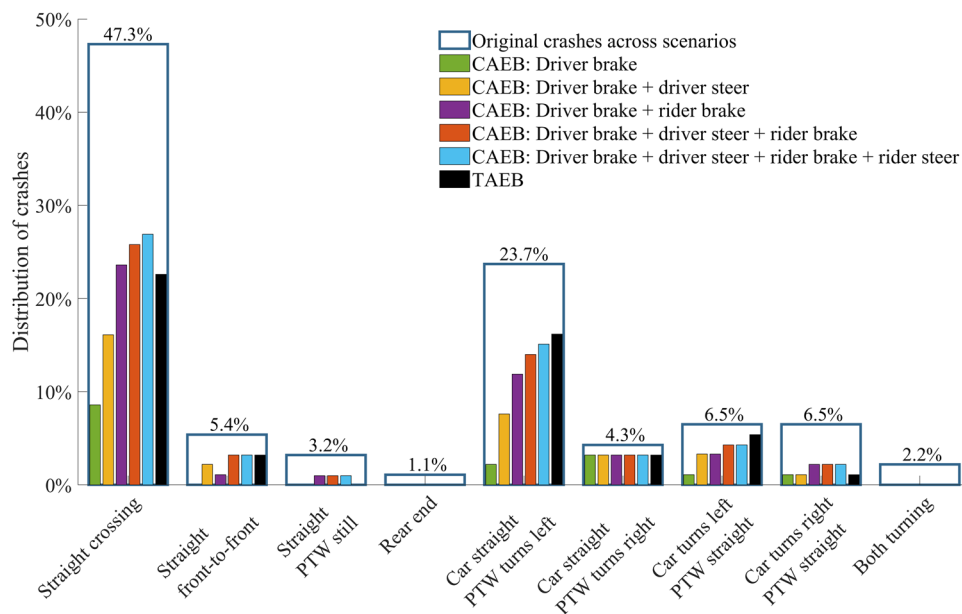


FIGURE A2 Distribution of original crashes (large transparent bars) and remaining crashes (small coloured bars) across the nine scenarios. Each coloured bar represents the proportion of the original 93 crashes that remains after that algorithm has been applied.

the percent of remaining crashes after each algorithm has been applied. The six algorithms show similar crash avoidance performances for the two most common scenarios, ‘Straight crossing’ and ‘Car straight, PTW turns left’. Across all scenarios, the CAEB: ‘Driver brake’ algorithm has the smallest proportion of remaining crashes, while the algorithm which includes the most comfortable avoidance opportunities (CAEB: ‘Driver brake + driver steer + rider brake + rider steer’), has the highest

proportion of remaining crashes for most scenarios. Where it is not the highest, the TAEB is—but only marginally.

The impact locations for each scenario’s remaining crashes for CAEB: ‘Driver Brake + Rider brake’ are shown in Figure A3. The two most common scenarios (‘Straight crossing’ and ‘Car straight, PTW turns left’) have similar impact location distributions—with 75–90% at the front corners, 10–25% at the front, and none at the vehicle sides. Understandably, the overall

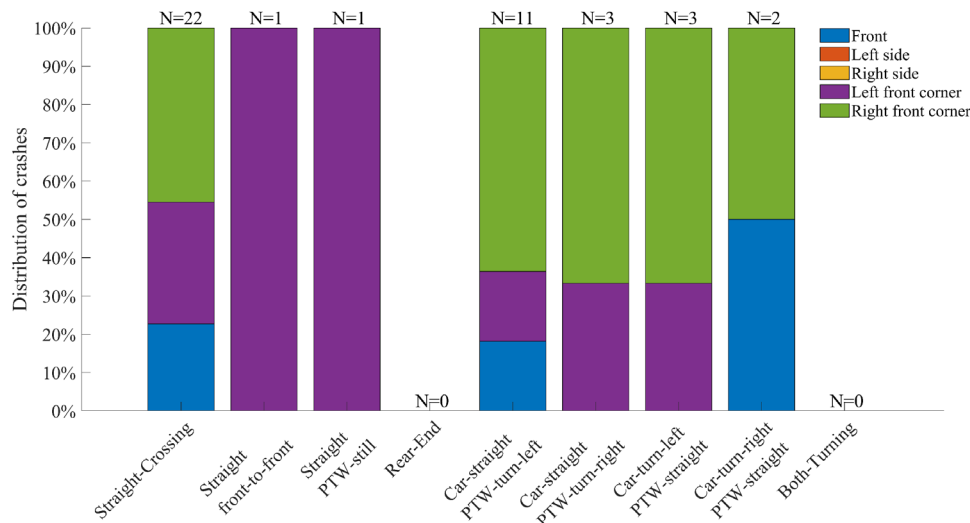


FIGURE A3 Distribution of impact locations across scenarios for CAEB: ‘Driver brake + rider brake’. The y-axis is the percent of the remaining crashes; the actual number of remaining crashes (N) is different for each scenario.

TABLE A1 Illustration pictograms of scenario classification.

Scenario type	Scenario illustration
Straight-crossing	
Straight front to front	
Car straight, PTW still	
Rear end	
Car straight, PTW turns left	
Car straight, PTW turns right	
Car turns right, PTW straight	
Car turns left, PTW straight	
Car turns right, PTW turns left	
Car turns left, PTW turns right	

impact location distribution for this AEB algorithm is similar to the distributions of these two scenarios, since they represent the largest numbers of cases.

As the two largest groups contain approximately two-thirds of the total number of crashes, the remaining seven contain very few; in fact, the largest remaining group, ‘car turns left, PTW straight’, contains only seven crashes. To reiterate, the small numbers make it problematic to compare the seven smaller groups, and we did not conduct rigorous statistical analyses of the differences in AEB performance across the different scenarios. But overall the crash distributions are similar across different scenarios.

**APPENDIX B
RATIONALE OF SENSOR CHARACTERISTICS
CHOICE**

The sensor FoV and range used in commercial AEB systems are not usually available. Jeppsson et al. [12] and Sui et al. [20] argue that the 40° FoV typically used for pedestrian AEB [15] must be substantially increased for intersections and two-wheelers. We did not want to choose a narrow FoV as we believe the FoV of future systems is likely to be substantially wider than today. Further, ranges used in previous literature vary substantially (e.g. 80 m in Uittenbogaard et al. [71] and 50 m in Char et al. [72]). We therefore chose a range somewhere in the middle of what is reported in the literature.

**APPENDIX C
KINEMATICS AND SHAPE PARAMETERS IN THE
SIMULATIONS**

The simulation framework uses point-mass kinematics; the kinematics parameters are described in Table C1.

The passenger car is represented as a rectangle with the two front corners cut off, and the PTW is represented as a rhombus (see Figure C1). The vehicle geometry definitions used in the virtual simulations (e.g. for crash avoidance calculations) are shown in Figure C1 and the parameters are described in Table C2.

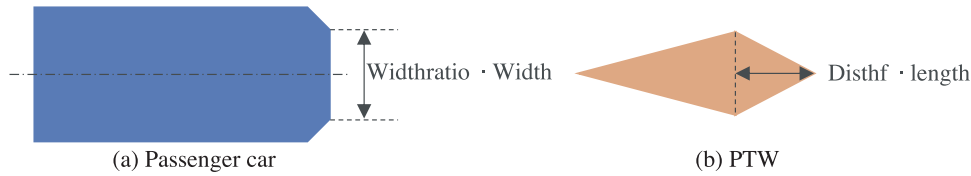


FIGURE C1 Vehicle geometries used in the virtual simulations.

TABLE C1 Kinematics parameter descriptions.

Kinematics parameters	Description
Position	The global x and y coordinates of the vehicle's centre of gravity. With the input of velocity, the change of position from one time step to the next is calculated.
Velocity	The driving speed of the vehicle. With the input of the longitudinal and lateral acceleration, the change in velocity from one time step to the next is calculated.
Acceleration	The driving longitudinal and lateral acceleration of the vehicle.
Heading angle	Driving direction of the vehicle in relation to the x -axis of the global coordinate system.
Yaw angle	The rotational angle around the vehicle's z -axis (vertical), representing its turning motion.

TABLE C2 Shape parameter descriptions for vehicle geometries. The parameters for each crash were provided as part of the SHUFO PCTSD.

Shape parameters	Description
Width	Width of the car and PTW, respectively
Length	Length of the car and PTW, respectively
Widthratio	Ratio to define width of leading edge for the passenger car
Disthf	Ratio to define distance handlebar to leading edge for the PTW.

An example of an original crash and the simulated AEB intervention can be found at the link <https://youtu.be/UYJh1o10jJA>.

APPENDIX D AUTOMATED EMERGENCY BRAKE ALGORITHM LOGIC

The logic of the TAEB and CAEB algorithms are shown in Figure D1; the naming conventions of Figure D1 are given in italics below, while the algorithm names are in quotation marks. Safety margins were incorporated into the (simulated) future predictions and the AEB algorithms by enlarging the shapes of the car and the PTW by a factor of 1.5 (e.g. making them 50% larger than the original shapes).

- *Initialize simulation*: is the start of the algorithm. Each time step in the simulation is 0.01 s.

- *Sensor model: Detect PTW*: Check if the PTW is in within the sensor FoV and range.
- *On collision course*: The path was predicted by extrapolating the current dynamics of the car and PTW (position, velocity, acceleration, heading angle, and yaw angle). The acceleration and yaw rate were assumed to be constant from the extrapolating point throughout the prediction-simulation.

The comfort-zone components (red diamonds) and the maximum-system-capability component (blue diamond) are the different algorithm components that are turned on or off for each CAEB system. For example, for CAEB: 'Driver brake + driver steer' only the *Driver brake avoid crash* and the *Driver steer avoid crash* components are turned on, while the remaining comfort algorithm components (in red) and the *Car brake avoid crash* (blue) are not active in that algorithm. The following describes the individual on/off algorithm components (red and blue). Note that all the red and blue models are evaluated independently. That is, using the predictive trajectory of the opponent's future path, each AEB system is simulated over time to find out if it is possible to avoid the crash comfortably (as defined by the longitudinal or lateral accelerations thresholds mentioned below).

- *Driver brake avoid crash*: The driver can brake comfortably (with a deceleration of less than 5 m/s^2) and still avoid a crash. The kinematics simulation used point-mass kinematics.
- *Driver steer avoid crash*: The driver can steer comfortably (with an absolute lateral acceleration of less than 5 m/s^2) and still avoid a crash. The kinematics simulation of the car used a bicycle model.
- *Rider brake avoid a crash*: The PTW rider can brake comfortably (with a deceleration of less than 5 m/s^2) and still avoid a crash.
- *Rider steer avoid crash*: The PTW rider can steer comfortably (with an absolute lateral acceleration of less than 5 m/s^2) and still avoid a crash. The kinematics simulation of the PTW used a bicycle model.
- *Car brake avoid crash*: This is the traditional AEB algorithm which simply checks if it is possible for the car to avoid a crash with a deceleration of 8.83 m/s^2 .

The *All On components have a No output* is then the final check of the algorithm. If all the active (turned on) components are No, the system will initiate braking with a deceleration of 8.83 m/s^2 .

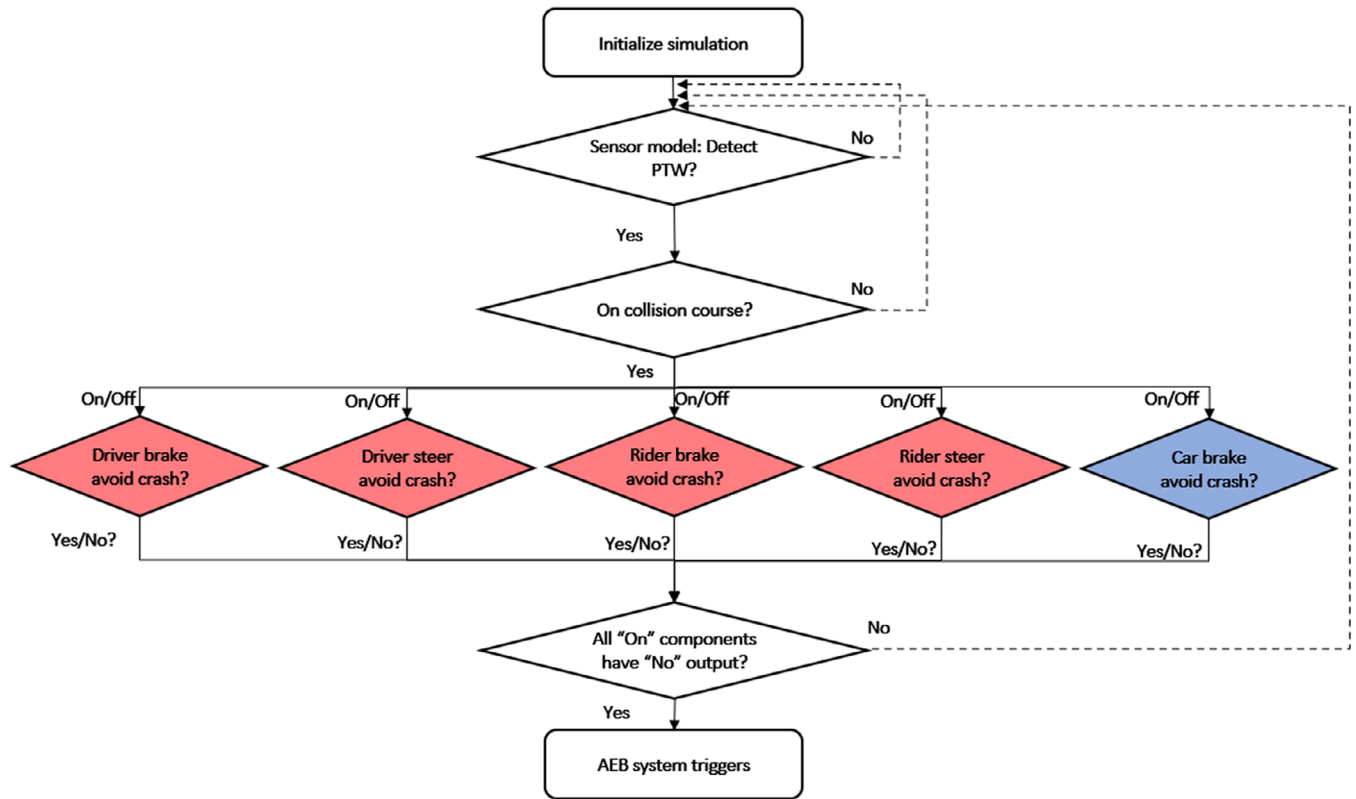


FIGURE D1 Flow chart of AEB algorithms.

TABLE E1 Parameters of injury risk level model [52].

Coefficients	MAIS2+F	MAIS3+F	Fatal
Intercept (β_0)	-2.256	-3.952	-7.175
Relative speed (β_1)	0.033	0.025	0.035
Impact on rider (β_2)	0.047	0.529	0.71

**APPENDIX E
THE INJURY RISK FUNCTION USED**

The injury risk reduction is calculated using the motorcyclist injury risk curve from Ding et al.'s work [52]; the risk model condition was the car impacting the side of the PTW. The input for the calculation is the relative impact speed, and the injury risk is calculated based on Equation (E.1). The coefficients for Equation (E.2) are taken from the same work (shown in Table E1, where β_0 is the intercept, β_1 the relative speed, and β_2 the impact on rider or not). The injury risk curve used is shown in Figure E1.

$$P(x) = \frac{1}{1 + e^{-t}} \tag{E.1}$$

$$t = \beta_0 + \beta_1 x_1 + \dots + \beta_n x_n \tag{E.2}$$

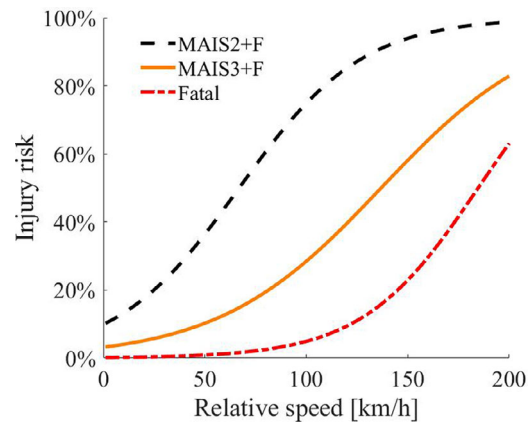


FIGURE E1 Motorcyclist injury risk curve.

The injury reduction effectiveness is calculated using Equation (E.3) [12], where N is the original crash injury risk and N' is the new injury risk for the remaining crashes after the application of each AEB algorithm, respectively.

$$E = \frac{N - N'}{N} \cdot 100\% = \left(1 - \frac{N'}{N}\right) \cdot 100\% \tag{E.3}$$